



MODELING THE GEOMETRY OF A FLAT END MILL IN TERMS OF THREE-DIMENSIONAL PARAMETERS

Dr. Rayapuri Ashok¹, G.Mallikharjuna², J.V.Mohanachari³

¹Professor & HOD, Department of Mechanical Engineering, Bheema Institute of Technology, Adoni, A.P. (India)

²Assistant Professor, Department of Mechanical Engineering, Bheema Institute of Technology, Adoni, A.P. (India)

³Research Scholar, Department of Mechanical Engineering, JNTUACEA, Ananatapuramu, A.P.(India.)

Abstract

End mills are widely used in industry for high-speed machining. End milling cutters are multi-point milling cutters with cutting edges both on the face end as well as on the periphery, and may be single or double end construction. The teeth of the cutter may be straight (parallel to the axis of rotation) or helical (at a helix angle). The cutter may be right-hand (to turn clockwise) or left-hand (to turn counter clockwise). The end mills have a straight or tapered shank for mounting and driving. Traditionally, the geometry of cutting tools has been defined using the principles of projected geometry (2D nomenclature) approach. The current work describes in detail the methodology to model the geometry of a flat end mill in terms of three-dimensional parameters. The proposed model defines the end mill in terms of three-dimensional rotational angles rather than the conventional two dimensional angles. **Keywords:** End mills, Machining, Milling cutters, Three-dimensional rotational angles.

1.INTRODUCTION

End mills combine the abilities of end cutting, peripheral cutting and face milling into one tool. End mills can be used on vertical and horizontal milling machines for a variety of facing, slotting, and profiling operations. End mills can be classified based upon:

(i) Configuration of end profile - Flat, Chamfer, Radius, Ball, Taper, Bull Nose end mills and their combinations.

(ii) Shank type – Screwed parallel shank, Plain shank, Weldon shank, Taper shank, Whistle notch parallel shank and Combination shank.

(iii) Mounting type - Cylindrical, Cylindrical threaded, Cylindrical power chuck, Weldon and Weldon threaded.

Geometry of cutting flutes and surfaces of end mills is one of the crucial parameters affecting the quality of the machining in the case of end milling. In the present work, the results of the generic definitions of flat end mills proposed by Tandon et al. [1] have been further developed, validated and applied for finite element analysis. Here, a generic flat end mill is modeled as it can be generalized to other types of end mills with complex shapes. A mathematical model of the geometry of a flat end mill is formulated in terms of its surface patches using the concept of surface modeling. The model is generated keeping in mind that it is to be used for direct analysis, prototyping, manufacturing and grinding of the cutters. The orientation of the surface patches is defined in a right hand coordinate frame of reference by three-dimensional angles, termed as rotational angles. The flutes of the flat end mill are modeled by sweeping the sectional profile of the cutter along the perpendicular direction. Mapping relations are developed between the proposed three-dimensional nomenclature and traditional two-dimensional (2D) projected geometry based nomenclatures. The output in the form of graphical model of the flat end mill is shown in OpenGL [2-3] for verification of the methodology. Besides, an interface is also

developed to directly pull the detailed mathematical / parametric definition of the end mill in a commercial CAD package for further validation (in the form of a solid model). This exact solid model is analyzed for static and transient dynamic load conditions. Also, the advantages offered by the detailed CAD model over an approximated CAD model are shown.

1.1 Surface Modeling of Flat End Mill

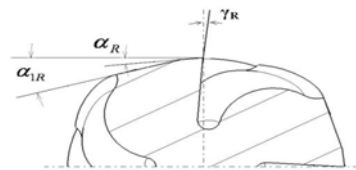
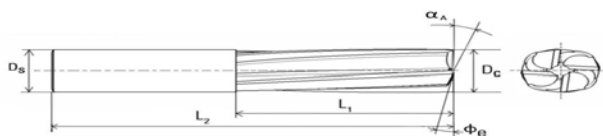
The geometry of a flat end mill projected on two-dimensional orthographic planes with its technical features is shown in Figure 1(a) and the sectional view of its flute is shown in Figure 1(b). L1 and L2 are the lengths of the fluted shank and the end mill respectively. Dc and Ds are the cutter diameter and shank diameter of the end mill respectively. For an endmill,

$\Sigma A, \Sigma e, \Sigma R, \Sigma 1R$ and ΣR are axial relief angle, end cutting edge angle, radial relief angle, radial clearance angle and radial rake angle respectively and are shown in Figure 1. The geometry of an end mill can be divided into three groups, namely

Geometry of fluted shank. End surface geometry. Shank geometry.

The fluted shank geometry consists of circumferential surface patches formed by helical sweeping a profile of a section of the fluted shank. The sweep operation is a combined rotational and parallel sweep, perpendicular to the axis of the cutter. The end geometry is dependent on the configuration of the flat end profile. A single tooth of a flat end mill may be modeled with the help of nine surface patches, labeled $\Sigma 1$ to $\Sigma 9$ as shown in Figure 2. They are Rake face ($\Sigma 1$), Peripheral land ($\Sigma 2$), ... Rake face extension ($\Sigma 9$). Shank geometry of the cutter may be a straight shank or tapered shank with surface patches modeled as axisymmetric surface of revolution along with a flat end surface

Figure 1: (a) Two-Dimensional Projected Geometry of a Flat End Mill



(b) Sectional View of End Mill Flutes

1.1.1 Modeling of Fluted Surface Geometry of End Mill

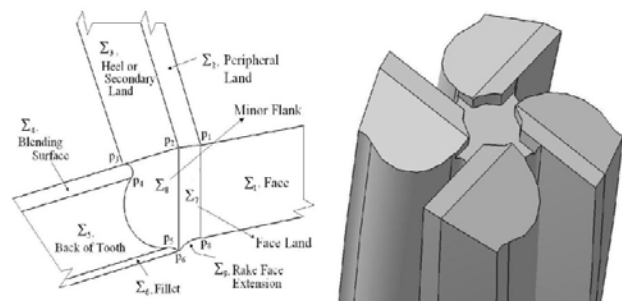


Figure 2 (a): Unfolded View of an End Mill Tooth .

Figure 2 (b): Tip Geometry of a Flat End Mill

Surfaces $\Sigma 1$ to $\Sigma 6$ are the surface patches on the fluted shank. These surfaces are formed when a composite curve in XY plane is swept with a sweeping rule, composed of combined rotational and parallel sweep, known as helicoidal surfaces. Figure 3 shows the composite sectional curve (V1...V7), consisting of six segments. Out of these six, three segments V1V2, V2V3 and V6V7 correspond to the three land widths, namely peripheral land, heel and face, and are shown as straight lines on a two-dimensional projected plane. The other three segments V3V4, V4V5 and V5V6 are circular arcs of radii r3, r2 and R respectively, corresponding to fillet, back of tooth and blending surface. The surface patches could better be visualized from the unfolded view of an end mill tooth (Figure 2 (a)). The tip geometry of the flat end mill is shown in Figure 2 (b). In modeling the cross-sectional profile of fluted shank in a two-dimensional plane, the input parameters are (i) widths of lands i.e. face, peripheral land and heel or secondary land given by l1, l2 and l3 respectively, (ii) 3D angles obtained to form face ($\gamma 1$), land ($\gamma 2$) and heel ($\gamma 3$) about Z axis, (iii) radii of fillet (R), back of tooth (r2) and blending surface (r3), (iv) diameter of cutting end of the end mill (Dc) and (v) number of flutes (N). The position

vectors of the end vertices of different sections of the composite profile curve (V1...V7) and center points of the three circular arcs (c1 , c2 , c3) are evaluated to parametrically model the profile curve.

The cross-sectional profile of a fluted section of an end mill consists of three parametric linear edges and three parametric circular arcs, namely, p1(s) to p6(s) . Edges p1(s), p2(s) and p6(s) are straight, while p3(s), p4(s) and p5(s) are circular in two-dimensional space. The generic definition of the sectional profile pi (s) in XY plane in terms of parameters may be represented by

$$p_i(s) = [f_1(s) \quad f_2(s) \quad 0 \quad 1]^T$$

The fluted surface is obtained by combined rotational and parallel sweeping and is parametrically described by

$$p(s, \phi) = p(s) \cdot [T_s], \text{ where transformation matrix is } [T_s]$$

$$[T_s] = \begin{bmatrix} \cos \phi & \sin \phi & 0 & 0 \\ -\sin \phi & \cos \phi & 0 & 0 \\ 0 & 0 & 1 & 0 \\ 0 & 0 & \frac{P\phi}{2\pi} & 1 \end{bmatrix} \text{ for } 0 \leq \phi \leq \frac{2\pi L}{P}$$

In the above equation, L1 is the length of fluted shank for flat end mills, φ be the parameter denoting the angular movement and P .is the pitch of the end mill.

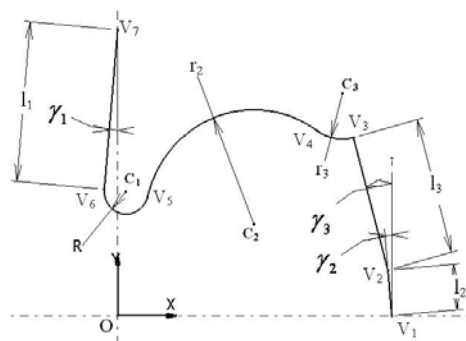


Figure 3: Composite Sectional Curve of an End Mill Flute

2.Sweeping rules:

The fluted section of an end mill can have right helix or left helix. If the flute's spiral has a clockwise contour when looked

along the cutter axis from either end, then it is a right helix else the helix is left [5-6]. For a right helix cutter, the cross-section curve rotates by an angle +φ about the axis in right hand sense. Three different sweeping rules can be formulated for the fluted shank and the end profile of the cutter. These rules are for

- (i) Cylindrical Helical Path
- (ii) Conical Helical Path
- (iii) Hemispherical Helical Path

2.1Cylindrical Helical Path :

The path when the composite profile curve is swept helically along a cylinder is known as cylindrical helical path. For a helical cutter let φ be the parameter denoting the angular movement, P the pitch of the helix, Dc the cylindrical cutter diameter and L1 the length of the fluted part of cutter, then the mathematical definition of the helix is

$$\begin{aligned} x &= (D_c / 2) \cos \phi \\ y &= (D_c / 2) \sin \phi \\ z &= (P\phi) / (2\pi), \text{ where } 0 \leq \phi \leq (2\pi L_1 / P) \dots\dots[1] \end{aligned}$$

2.2Conical Helical Path –

The helical path along a frustum of cone of cutting end diameter Dc and shank side diameter Ds is defined by

$$\begin{aligned} x &= (D / 2) \cos \phi \\ y &= (D / 2) \sin \phi \\ z &= (P\phi) / (2\pi), \text{ where } D = D_c + (D_c - D_s)z / L_1 \text{ and } 0 \leq \phi \leq (2\pi L_1 / P). \dots\dots[2] \end{aligned}$$

This is valid for both types of frustum of cones i.e. when Dc < Ds and when Dc > Ds

2.3.Hemispherical Helical Path –

The helical path along the hemispherical object of diameter Dc is given as

$$\begin{aligned} x &= (D / 2) \cos \psi \cos \phi \\ y &= (D / 2) \cos \psi \sin \phi \\ z &= (D_c / 2)(1 - \sin \psi), \text{ where } 0 \leq \phi \leq \pi D_c / P \text{ and } 0 \leq \psi \leq \pi / 2. \dots\dots[3] \end{aligned}$$

Here, α is the angle about Z axis and β is the angle with XY plane and the relation

$$\begin{aligned} \text{between } & \alpha \text{ and } \beta \\ \text{them is, } & \tan \alpha = \frac{D}{c} \\ & \sin \beta = \frac{c}{D} \end{aligned}$$

3.Mapping Relations:

In this work, relations to map the proposed 3D rotational angles, used to define the geometry of the flat end mills, into conventional 2D projected angles and vice versa are developed. The former is called forward mapping while the latter is known as inverse mapping [1]. The conventional angles are formed by projecting the surface patches of the end mill on planes of projection and the traditional geometry of end mill can be referred in the literature [5,6 7, 8,]. Table 1 shows the forward mapping relations for a flat end mill. The solution of these forward mapping relations establishes inverse mapping that helps to evaluate the 3D rotational angles if tool angles specified by conventional nomenclatures are known. Table 2 presents the inverse mapping for an end mill.

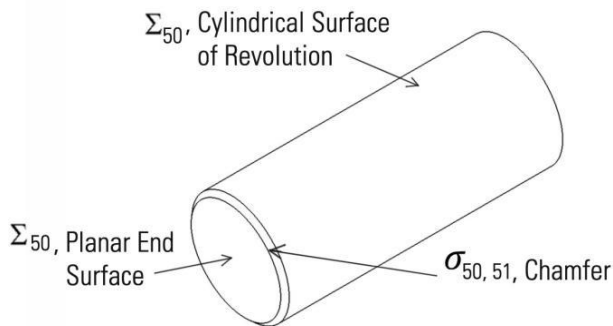


Figure 4: Modeling of Shank

4.Modeling Algorithm:

Based on the above proposed generic definition, the parameters needed to completely describe a four-flute helical flat end mill and the relevant data for these parameters to exemplify the methodology are shown in Table 2.3(a) and 2.3(b). The algorithm that geometrically models a fluted helical end mill based on the proposed three-dimensional nomenclature (3D rotational

angles and other dimensional parameters) is as follows:

Step 1: The composite sectional curve of the flute in two-dimensional Cartesian coordinate plane, with center of the flat end mill's cross section coinciding with global origin is generated as described in Section 1.1.

Step 2: The solid flute is generated by combined rotational and parallel sweeping of composite sectional curve as illustrated in Section 1.1.

Step 3: The end geometry of flat end mill is formed through Boolean operations on the surface patches and the blending surfaces as mentioned in Section 1.2.

Step 4: The Shank is generated by applying Boolean operation on surface patches Σ_{50} and Σ_{51} , and blending surface ($\Sigma_{50,51}$) as mentioned in Section 1.3.

Step 5: The detailed and complete CAD model of the end mill is generated.

The details of the implementation depend on the specific CAD environment, where they are implemented, and are discussed in Section 4.

Table 3(a): Geometric Parameters (Dimensional) and Input Data for an End Mill

Rotational Angles	Value (degrees)
α_1	-5.0
α_2	10.0
α_3	20.0
α_7	70.0
Helix angle (α)	30.0

5.Implementation of Algorithm:

The algorithm has been implemented in OpenGL environment [9], a general purpose graphical modeling kernel, as well as in a commercial CAD environment (here, CATIA V5) [10-11]. The rendering of the end mill cutter (input data as in Table 2.3(a) and 2.3(b)) by using the 3D parameters proposed in the work, directly in OpenGL and CATIA V5, validates the modeling methodology

5.1Implementation in Open GL Environment:

OpenGL is an Application Programming Interface (API). It is graphical software that uses boundary representations to describe models. To directly render the helical flat end mill using 3D geometric parameters as proposed in this work, a tool design program is developed in C programming language. All geometric primitives are defined in terms of vertices. The 3D geometric parameters were supplied as input in a text file. The program developed in C easily call functions in the API for rendering. The libraries like GLU, GLX, GLUT, Open Inventor, etc, simplify our programming tasks for rendering the cutter in OpenGL. The output is the rendered image of the flat end mill in OpenGL graphical environment as shown in Figure 5(a). OpenGL file formats are used for rendering purpose only. It is difficult to accurately export the rendered image of OpenGL file format to a commercial CAD/CAE/CAM environment for any meaningful technological application.

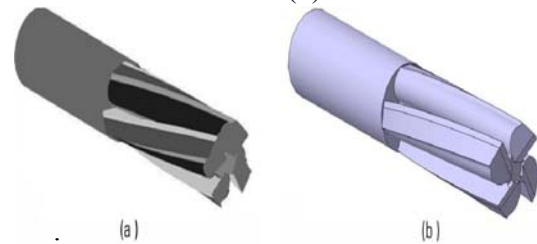
5.2 Implementation in Commercial CAD Environment

To fully utilize the accurate and comprehensive parametric definition of the cutter, there is a need to pull this model in a commercial modeling package so as to take advantages of the tools of the modeler for further processing. An interface is developed here to directly generate the model in a solid modeling environment (CATIA V5) using the comprehensive definition of the cutter. This leads to a wide range of downstream applications.

CATIA V5 is a commercial solid modeler that allows users to create 3D models in a Graphical User Interface (GUI). Solid models can also be created using Visual Basic function calls through an application programming interface (API) [12]. A Visual Basic, C++ program is developed here that uses this API to generate the model of the helical flat end mill based on the user defined 3D geometric parameters directly in CATIA. The model is not created using the GUI of the software but uses the parametric definitions of the surfaces developed, as described in Section 2.1. The users can change the geometric parameters of the end mill in a custom developed user interface and based on the chosen parameters, the end mill model is directly generated in CATIA modeling environment (as shown in Figure 2.5(b)). Using

the GUI, if one has to create another model for a different set of parameters, one has to rebuild the model, may be, from scratch. With the parametric definitions and the interface developed here, the user can create a set of models by simply changing the input values. It is possible to save the geometric model of the end mill in a variety of file formats, including CAT PART, IGES, and STL. The CATIA implementation gives more control to the user because the end mill is modeled directly in a modeling environment where further modifications and embellishments can be easily done.

Figure 5: Rendering of an End Mill in (a) OpenGL environment and (b) CATIA V5



Dimensional Parameters	Values
Number of flutes (N)	4
Cutter diameter (D_C)	25.0 mm
Length of cutter (L_2)	131.0 mm
Length of flutes (L_1)	71.0 mm
Root diameter (D_R)	21.0 mm
Shank side diameter (D_S)	25.0 mm
Pitch (P)	450.0 mm
Width of primary land (l_2)	2.0 mm
Width of heel (l_3)	6.0 mm
Width of rake face (l_1)	7.0 mm
Fillet Radius (R)	1.0 mm
Radius of back of tooth (r_2)	5.0 mm
Radius of blending surface (r_3)	2.0 mm

6. Application of Helical Flat End Mill Models:

Numerous technological downstream applications may be performed on the geometric models of the helical flat end mill cutters developed by the above defined technique. One such technological application is finite element based engineering analysis (FEA) of the end mill. This section presents an exercise on FEA on the 3D model of the helical end mill. This exercise highlights the advantages and utilities available, once a comprehensive.

3D definition of the cutter is available. The purpose here is not to present any detailed analysis of the end mill during machining. The end mills are generated in CATIA as described in Section 2.4.2 and exported to Generative Structural Analysis module in CATIA Analysis and Simulation package for Structural Static and Transient Dynamic Analysis. For the accuracy of simulation, the cutting force data taken in the work are based on results of the cutting tests conducted by Li et al. [13]. For our simulation, we have chosen the cutter material and the cutting conditions as follows:

- Cutter: A four-fluted M42 High Speed Steel with a helix angle $\alpha = 30^\circ$ and other geometric parameters as mentioned in Table 2.3.
- Material properties of the High Speed Steel cutter : It is Molybdenum based high speed steel with Weight % of C = 1.05-1.15, Mn = 0.15-0.40, Si = 0.15-0.65, Cr = 3.50-4.25, Ni = 0.3, Mo = 9.00-10.00, W = 1.15-1.85, V = 0.95-1.35, Co = 7.75-8.75, Cu = 0.25, P = 0.03, S = 0.03. It is an isotropic material with Young's modulus = 2.1×10^{11} N/m², Poisson's ratio = 0.3, density = 7980 kg/m³, thermal expansion = 1.33×10^{-5} K and tensile strength = 970N/mm².
- Work piece: Plain carbon steel which has a chemical composition of approximately 0.5% C, 0.5% Mn, 0.25% Si.
- Cutting Parameters: Axial depth of cut 12 mm, spindle speed 600 rpm, feedrate 240 mm/min i.e. the feed per tooth per revolution = 0.1 mm

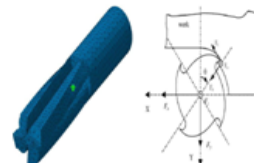
The end mill is meshed using parabolic tetrahedral elements. The tetrahedral element is a ten node iso-parametric solid element having 3 (translational) degrees of freedom. It has a quadratic displacement behavior and is well suited to model irregular meshes. Quadratic tetrahedral (QT) element is preferred for the development of smooth automatic mesh FE model for the geometry of complex solid

models like femur, fluted cutters, etc.. For automatic mesh generation, meshes comprising entirely of tetrahedral elements (or all-tetrahedral mesh) are frequently generated as opposed to a mesh comprising of purely hexahedral elements (or all-hexahedral mesh). This is because a physical domain, as in the case of geometrically complex structures, cannot always be decomposed into an assembly of hexahedral elements. It can however be easily represented as a collection of tetrahedral elements, as these elements are geometrically more versatile. Infact, performing FEA using QT mesh models is efficient in terms of both accuracy and CPU time. Also, QT finite element models are more stable and less influenced to the degree of refinement of the mesh, when modeling complex solids. The element also has plasticity, creep, swelling, stress stiffening, large deflection, and large strain capabilities. The meshing information of the end mill is presented in Table 4. Figure 6 shows the finite element mesh of the end mill cutter. The next step is to restrain the end mill model by clamping the shank of the tool followed by load application.

For our simulation, load has been applied on a single flute in radial, tangential and axial directions for an axial depth of 12mm. Figure 7 shows the coordinate system and the cutting force direction on the flute of the end mill cutter. The simulated and measured cutting forces in the time domain of two revolutions of cutter rotation as worked out by Li et al. [13] is shown in Figure 8. Using the cutting forces mentioned in Figure 8, the forces acting in radial, tangential and axial directions on the end mill flute can be calculated from the angle domain convolution integral theory mentioned by Zheng et al.

Table 4: Meshing Information of an End Mill Cutter

Parameters	Values
Global mesh size	7 mm
Local mesh size	1mm
Jacobian	0.3
Nodes	42289
Elements	27164
Warp	60
Absolute sag	0.3 mm
Proportional sag	0.2 mm



7. Structural Transient Dynamic Analysis:

For transient dynamic analysis, only time factor has been considered. Vibrations and other dynamic factors are not included in this work. The transient dynamic analysis is carried out for a total time domain of 0.025 sec (for cutter angle rotation of 90°), with a time interval of 0.005 sec. Table 2.5 shows the forces acting on the flute for a time profile of 0.0025 sec. Figures 12, 13 and 14 shows the result for transient dynamic analysis with Von mises stress, deformed mesh and translational displacement respectively for the applied load. For the dynamic case, the result shown is maximum equivalent stress of 978 MPa and maximum total displacement of 0.0455 mm at time 0.015 sec.

Table 2.5: Forces Acting on a Particular Flute of a Helical End Mill

θ	Time (sec)	F_t (N)	F_r (N)	F_a (N)
0°	0.00	297.5	169.82	61.18
36°	0.01	510.0	190.0	77.5
54°	0.015	269.29	229.11	66.906
72°	0.02	236.25	252.0	70.875
90°	0.025	210.0	140.0	40.25

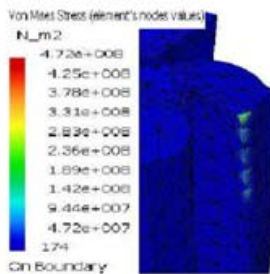
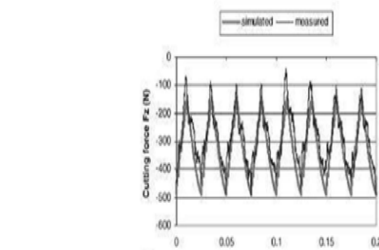
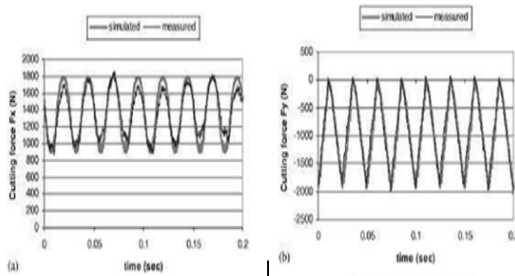


Figure 9: Von Mises Stress for Static Load Condition

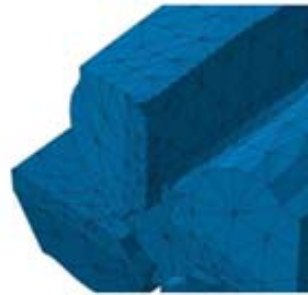


Figure 10: Deformed Mesh for Static Load Condition

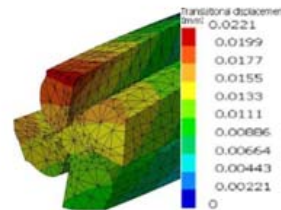


Figure 11: Translational Displacement for Static Load Condition

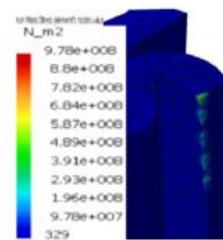


Figure 12: Von Mises Stress for Transient Dynamic Load Condition at 54°

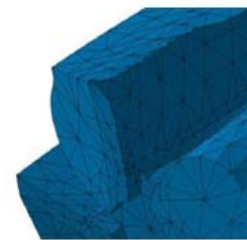
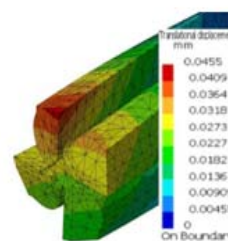


Figure 13: Deformed Mesh for Transient Dynamic Load Condition at 54°



8. Results and Discussions:

This Section highlights the advantages offered by the detailed CAD model over an approximated CAD model. Figure 15 shows an approximated CAD model with one of its flute, analyzed for finite element simulation under the load conditions at cutter angle rotation (\square) of 36° (same as for exact CAD model). Using the analytical cutting force model and stress relationships for end milling operations, described by Chiou et al. [14] and Armarego

etal. [15], the shear stresses are calculated at one of the cutting flutes under the load conditions. Table 2.6 presents the values of shear stresses calculated analytically as well as that obtained by performing finite element simulation on the same flute using approximated CAD model and detailed CAD model. The analytical values of the shear stress are compared with the finite element simulation results of the two types of CAD models at $\phi = 32^\circ$ and $\phi = 36^\circ$. The difference in the values of the shear stresses between the analytical and two finite element computations is tabulated in the form of error analysis in Table 2.6. The error analysis proves that the results of the FEA simulation on the detailed CAD model are closer to the analytical data than the results of approximated CAD model. It has also been observed while performing the finite element analysis using the approximate CAD model that the stress values sharply overshoots at some points on the cutter flute as shown at the tip of cutting edge (Table 6). This may be due to the fact that approximate CAD model approximates the geometry at certain locations. It is evident that the detailed CAD model is consistently in better agreement with the analytically calculated data rather than the approximated model and can lead to accurate design and fabrication of the cutters.

Table 6(a): Comparative Results of Finite Element Simulation at $\phi = 32^\circ$

	Analytical Shear Stress (MPa)	Approximated CAD Model			Detailed CAD Model		
		Von Mises Stress (MPa)	Error (%)	Translational Displacement (mm)	Von Mises Stress (MPa)	Error (%)	Translational Displacement (mm)
At tip of the cutting edge, Global Maxima	521.87	2950.2	465	0.0399	472.21	9	0.0221
At flank of the side cutting edge, Local Maxima 1 & 2	194.98	167.1	14	0.0359	178.4	8.5	0.0199
	92.9	144.9	55.9	0.0319	77.7	16.3	0.0177

Table 6(b): Comparative Results of Finite Element Simulation at $\phi = 36^\circ$

	Analytical Shear Stress (MPa)	Approximated CAD Model			Detailed CAD Model		
		Von Mises Stress (MPa)	Error (%)	Translational Displacement (mm)	Von Mises Stress (MPa)	Error (%)	Translational Displacement (mm)
At tip of the cutting edge, Global Maxima	1050.03	6199.3	490	0.0793	978.0	6.8	0.0455
At flank of the side cutting edge, Local Maxima 1 & 2	392.46	419.9	6.9	0.0714	376.6	4	0.0409
	182.23	346.2	89	0.0634	150.3	17.5	0.0364

9.conclusions

Traditionally, the geometry of cutting tools has been defined using the principles of projected geometry (2D nomenclature) approach. This

chapter describes in detail the methodology to model the geometry of a flat end mill in terms of three-dimensional parameters. The proposed model defines the end mill in terms of three-dimensional rotational angles rather than the conventional two dimensional angles. The model is validated while rendering the cutter directly in OpenGL environment in terms of three dimensional parameters. Further, an interface is developed that directly pulls the proposed three-dimensional model defined with the help of parametric equations into a commercial CAD modeling environment (here CATIA V5). Besides, the modeled tool is used for finite element simulations to study the cutting flutes under static and transient dynamic load conditions. The results show that the methodology offers a simple and intuitive way of generating accurate surface models for use in machining process simulations

REFERENCES

- [1] Tandon, P., Gupta, P. & Dhande, S.G., 2008, Geometric Modeling of Fluted Cutters, ASME Journal of Computing and Information Science in Engineering, 8, pp. 021007-1-15.
- [2] Woo, M., Neider, J. & Davis, T., 1998, OpenGL Programming Guide, 2nd ed., Addison-Wesley, Reading, MA.
- [3] Wright Jr., R.S. & Sweet, M., 2000, OpenGL SuperBible, Techmedia (Waite Group Press), New Delhi..
- [4] Alves, M.L., Fernandes, J.L.M., Rodrigues, J.M.C. & Martins, P.A.F., 2003, Finite Element Meshing in Metal Forming using Hexahedral Elements, Journal of Materials Processing Technology, 141, pp. 395-403.
- [5] Dallas, D.B., 1976, Tool and Manufacturing Engineers Hand book, [25] 3rd ed., McGraw-Hill, New York.
- [6] Ehmann, K.F., 1990, Grinding Wheel Profile Definition for the Manufacture of Drill Flutes, Annals of the CIRP, 39(1), pp. 153-156.
- [7] Warkhedkar, R.M. & Bhatt, A.D., 2008, Material-Solid Modeling of Human Body: A Heterogeneous B-Spline based Approach, Computer-Aided Design, DOI:10.1016/j.cad.2008.10.016.
- [8] Zheng, Li., Chiou, Y.S. & Liang, S.Y., 1996, Three Dimensional Cutting Force Analysis in End Milling, International

- Journal of Mechanical Sciences,**38**(3), pp. 259-269.
- [9] Yau, H.T. & Tsou, L.S., 2009, Efficient NC Simulation for Multi-Axis Solid Machining With a Universal APT Cutter, ASME Journal of Computing and Information Science in Engineering,**9**, pp. 021001-10.
- [10] Tickoo, S. & Ekbote, S., 2007, CATIA V5R15 for Engineers & Designers, Dreamtech Press, New Delhi
- [11] Zhang, Z., Zheng, L., Li, Z., Liu, D., Zhang, L. & Zhang, B., 2003, A Cutting Force Model for a Waved-Edge End Milling Cutter, International Journal of Advanced Manufacturing Technology, **21**, pp. 403-410.
- [12] Cidoncha, M.G.D.R, Palacios, J.M. & Ortiz, F.O., 2007, Task Automation for Modelling Solids with Catia V5, Journal of Aircraft Engineering and Aerospace Technology, **79**(1), pp. 53-59.
- [13] Li, H.Z., Zhang, W.B. & Li, X.P., 2001, Modelling of Cutting Forces in Helical End Milling using a Predictive Machining Theory, International Journal of Mechanical Sciences,**43**, pp.1711-1730.
- [14] Chiou, C.H., Hong, M.S. & Ehmann, K.F., 2005, Instantaneous Shear Plane Based Cutting Force Model for End Milling, Journal of Materials Processing Technology,**170**, pp. 164-180.
- [15] Carlsson, T. & Stjernstoft, T., 2001, A Model for Calculation of the Geometric Shape of the Cutting Tool-Workpiece Interface, Annals of the CIRP,**50**(1), pp. 41-44